MOLECULAR AND CELLULAR BIOLOGY, Aug. 2004, p. 6811–6823 Vol. 24, No. 15
0270-7306/04/$08.00+0 DOI: 10.1128/MCB.24.15.6811–6823.2004

SMU-2 and SMU-1, *Caenorhabditis elegans* Homologs of Mammalian Spliceosome-Associated Proteins RED and fSAP57, Work Together To Affect Splice Site Choice

Angela K. Spartz, Robert K. Herman, and Jocelyn E. Shaw*

Department of Genetics, Cell Biology and Development, University of Minnesota, Minneapolis, Minnesota 55455

Received 16 October 2003/Returned for modification 13 January 2004/Accepted 20 April 2004

Mutations in the *Caenorhabditis elegans* gene *smu-2* suppress *mec-8* and *unc-52* mutations. It has been proposed that MEC-8 regulates the alternative splicing of *unc-52* transcripts, which encode the core protein of perlecan, a basement membrane proteoglycan. We show that mutation in *smu-2* leads to enhanced accumulation of transcripts that skip exon 17, but not exon 18, of *unc-52*, which explains our finding that *smu-2* mutations suppress the uncoordination conferred by nonsense mutations in exon 17, but not in exon 18, of *unc-52*. We conclude that *smu-2* encodes a ubiquitously expressed nuclear protein that is 40% identical to the human RED protein, a component of purified spliceosomes. The effects of *smu-2* mutation on both *unc-52* pre-mRNA splicing and the suppression of *mec-8* and *unc-52* mutant phenotypes are indistinguishable from the effects of mutation in *smu-1*, a gene that encodes a protein that is 62% identical to human spliceosome-associated protein fSAP57. We provide evidence that SMU-2 protects SMU-1 from degradation in vivo. In vitro and in vivo coimmunoprecipitation experiments indicate that SMU-2 and SMU-1 bind to each other. We propose that SMU-2 and SMU-1 function together to regulate splice site choice in the pre-mRNAs of *unc-52* and other genes.

The excision of introns from pre-mRNA is carried out by the spliceosome, a complex machine composed of five snRNAs and many—approximately 145 in humans (52)—different proteins. Understanding how the spliceosome regulates splicing and splice site choice is complicated by the phenomenon of alternative RNA splicing, in which a given transcript can be spliced in alternative ways to generate different mRNA isoforms, which may be translated into different protein products with different functions (2). In a few cases, alternative splicing factors that regulate the alternative splicing of specific pre-mRNA targets in a development- or tissue-specific manner are known. Well-studied examples include the *Drosophila melanogaster* Sxl, Tra, and Tra2 proteins, which regulate alternative splicing of genes involved in fly sex determination.

The *Caenorhabditis elegans* protein MEC-8 also behaves as a specific regulator of alternative splicing. It contains two RNA recognition motifs and promotes the accumulation of two alternatively spliced isoforms of *unc-52* pre-mRNAs (29). *mec-8* null mutants are viable and fertile but exhibit defects in mechanosensation, chemosensation, and embryogenesis (7, 28), which have been attributed to defects in the processing of pre-mRNA targets of MEC-8 action other than *unc-52* (28, 43). The specific phenotypes conferred by *mec-8* mutation along with the tissue-specific pattern of *mec-8* expression (42) suggest that MEC-8 is a specific rather than general regulator of splicing, and no apparent orthologs of MEC-8 have been found in purified human spliceosomes.

* Corresponding author. Mailing address: Department of Genetics, Cell Biology and Development, University of Minnesota, 6-160 Jackson Hall, 321 Washington Ave. SE, Minneapolis, MN 55455. Phone: (612) 625-1912. Fax: (612) 624-8118. E-mail: jocelyn@biosci.cbs.umn.edu.

MEC-8's action on *unc-52* transcripts accounts for a synthetic lethal interaction exhibited by *mec-8* mutations when they are combined with those for any of several otherwise-viable alleles of *unc-52*. The *unc-52* gene encodes the *C. elegans* homolog of the protein core of mammalian perlecan, a heparan sulfate proteoglycan found in basement membranes (38). Null mutations in *unc-52* prevent assembly of the myofilament lattice of body wall muscle during embryogenesis and result in paralysis and arrest at the twofold stage of embryonic elongation (38), a phenotype characteristic of nonfunctional muscle (49). Exons 16, 17, and 18 of *unc-52*, each of which encodes a single immunoglobulin repeat, are alternatively spliced to generate slightly different UNC-52 isoforms (34, 37, 38). Viable mutations in this alternatively spliced region, including nonsense mutations in exons 17 and 18, do not seem to affect embryogenesis or early larval development but cause later progressive loss of muscle attachments to the adjoining basement membrane, hypodermis, and cuticle, resulting in a late-onset paralysis (37). The phenotypic effect of the *unc-52* viable mutations is greatly enhanced by loss-of-function *mec-8* mutations, such that *mec-8*; *unc-52*(*viable*) embryos resemble *unc-52* (null) embryos (28, 29). MEC-8 has been shown to be required to generate *unc-52* mRNA isoforms that splice exon 15 to exon 19 and that splice exon 16 to exon 19 (29). Thus MEC-8 is needed to generate the isoforms that skip exons containing *unc-52* viable mutations and that provide enough UNC-52 function for embryogenesis and early larval development of these *unc-52* mutants.

We have taken a genetic approach to identifying new genes affecting alternative splicing. A temperature-sensitive *mec-8* mutation was combined with a temperature-sensitive *unc-52* viable mutation to yield a temperature-sensitive synthetic lethality. Recessive, loss-of-function suppressors of this synthetic

lethality were identified as two genes, *smu-1* and *smu-2* (*smu* for suppressor of *m*ec-8 and *unc-52*) (28). In addition to suppressing the *mec-8*; *unc-52*(*viable*) synthetic lethal interaction, *smu-1* and *smu-2* mutations suppress the late-onset paralysis conferred by certain *unc-52* viable mutations and provide a weak bypass suppression of the pleiotropic effects of *mec-8* mutations, suggesting that *smu-1* and *smu-2* affect the alternative splicing of a number of pre-mRNAs. Apart from mildly deleterious effects on mobility, growth, and brood size, *smu-1* and *smu-2* mutations confer no obvious phenotype on their own. The *smu-1* gene was characterized molecularly and shown to encode a WD repeat protein with more than 60% identity to a human protein of unknown function (43). More recently, the human protein was shown to be a component of the spliceosome (52).

In this paper we describe the genetic and molecular characterization of *smu-2*. We have found that *smu-2* mutations confer the same phenotype as mutations in *smu-1* (43). *smu-2* mutations interact with specific alleles of *unc-52*, and these interactions can be explained by changes in the relative abundance of *unc-52* alternatively spliced transcripts. We have cloned the *smu-2* gene and found that it encodes a highly conserved protein, the homolog of human RED, which has been isolated in purified human spliceosomes (35, 52). SMU-2 is a nuclear, ubiquitously expressed protein. We also show that SMU-2 interacts with SMU-1 in vitro and in vivo and that this interaction seems to be required to stabilize SMU-1. We propose that SMU-1 and SMU-2 bind to each other as components of the spliceosome and modulate splice site selection of many pre-mRNAs.

MATERIALS AND METHODS

Genetic methods, genes, and alleles. Nematode culturing and genetics were performed as described previously (4, 45). Crosses involving *unc-52*(*e669su250ts*), which we refer to as *unc-52*(*ts*), were done at 25°C; all other crosses were done at 20°C. Except for RC301 (15), whose use is described in the next section, all strains were derived from the wild-type Bristol stock N2. Previously identified genes and mutations used in this work were as follows: LGI (linkage group I), *mec-8*(*u218*), *smu-1*(*mn415*), *unc-101*(*m1*); LGII, *smu-2*(*mn416*, *mn610*, *mn611*), *unc-52*(*e1421*, *e669su250*, *e669*, *e1012*, *e444*, *e998*), *lin-31*(*n301*); LGIII, *unc-36* (*e251*); LGV, *him-5*(*e1490*).

Genetic and physical mapping of *smu-2*. To obtain a genetic map distance between *smu-2* and *lin-31*, non-Unc-52 (recessively suppressed) progeny of *smu-2*(*mn416*) *lin-31 unc-52*(*ts*)/+ + *unc-52*(*ts*) hermaphrodites were picked and scored for the recessive Muv phenotype conferred by *lin-31*. Since *lin-31* is incompletely penetrant, genotypic assignments were confirmed by scoring the phenotypes of self progeny of picked animals. Four Smu non-Lin-31 recombinants were obtained from a total of 475 non-Unc-52 animals, giving a *smu-2*-to-*lin-31* map distance of about 1 centimorgan (cM) after correcting for growth at 25°C (39).

We used DNA dimorphisms between RC301 and N2 to situate *smu-2* on the physical map (17). Four dimorphisms were identified by amplifying DNA by PCR and finding differences in the sizes of PCR products made from N2 and RC301 DNA. A fifth dimorphism, *mnP5*, was identified as a single nucleotide difference between sequenced PCR products. The primers used to identify the five dimorphisms, their locations on the physical map, and their corresponding differences in PCR size or nucleotide sequence are as follows. For *mnP1* primer A was GGATTCTGGTTGTGATGACACG, primer B was GTATAGCCATTCCTCG ATGTGG, the cosmid was ZC239, the N2 product was 1,009 bp, and the RC301 product was 900 bp; for *mnP2* primer A was AGGAGCTGAGCAAGATTGCC, primer B was TATTGCACACCGAGGAGACC, the cosmid was F53C3, the N2 product was 867 bp, and there was no product for RC301; for *mnP3* primer A was GAACGACCTAATAGTTTGTGCTCG, primer B was AAAGAGTCAACCT GAACTCGC, the cosmid was W09G10, the N2 product was 1,226 bp, and the RC301 product was ≈ 1,100 bp; for *mnP4* primer A was TCACTATTCTCAG CGTTCTCTCC, primer B was CCAGTTGTCTTCACCTACGTCC; the yeast artificial chromosome (YAC) was Y49F6B, the N2 product was 1,442 bp, and the RC301 product was ≈ 1,375 bp; for *mnP5* primer A was ACAGCCTTTATGT CGTTGGC, primer B was GTTCTGGAACATGATGCTGC, the cosmid was C16C8, and at position 40014 the N2 product was T and the RC301 product was C. Recombinants were mapped for the presence of these RC301 dimorphisms using single worm PCR assays (48). For *mnP2*, an unrelated PCR was done in the same tube as a control to ensure that DNA was present in the sample.

To map *smu-2* with respect to the DNA dimorphisms, we first made a strain containing DNA sequence in the *smu-2* region from RC301 coupled to *unc-52*(*ts*) by crossing RC301 males with *lin-31 unc-52*(*ts*) hermaphrodites and picking Unc-52 F_2 progeny that did not segregate *lin-31*. We confirmed by PCR that this stock contained the five RC301 dimorphisms used in our mapping. To obtain recombinants for mapping, we crossed *smu-2*(*mn416*) *lin-31 unc-52*(*ts*)/+ males to the RC301-marked *unc-52*(*ts*) hermaphrodites, and from F_1 Unc-52 cross progeny that segregated Muv non-Unc-52 self progeny, we picked non-Muv non-Unc-52 recombinants, genotype *smu-2 unc-52*(*ts*)/*smu-2 lin-31 unc-52*(*ts*). Homozygous *smu-2 unc-52*(*ts*) recombinants were recovered and scored with respect to the dimorphisms. The five dimorphisms are all situated left of *lin-31* on the physical map in the left-to-right order as *mnP1*, *mnP5*, *mnP4*, *mnP3*, and *mnP2*. Out of 26 total recombinants, no crossovers occurred between *mnP1* and *mnP5*, three occurred between *mnP5* and *mnP4*, two occurred between *mnP4* and *mnP3*, 16 occurred between *mnP3* and *mnP2*, and 5 occurred between *mnP2* and *lin-31*. Subsequent cloning of *smu-2* confirmed that it lies between *mnP5* and *mnP4*. We also mapped the left end point of the deficiency *ccDf1*, which deletes *lin-31* and which complements *smu-2*. Arrested embryos of *ccDf1*/+ parents were scored for the presence of N2-type PCR products. We found that *ccDf1* ends between *mnP4* and *mnP3*.

Genetic interactions. *smu-2* was tested for interactions with a variety of *unc-52* viable mutations, either alone or in combination with *smu-1*. To construct *smu-2 unc-52* strains, *lin-31 unc-52* mutants were generated for each *unc-52* allele and crossed to homozygous *smu-2* males. Cross progeny were allowed to produce self progeny, and Unc-52 non-Muv recombinants of genotype *smu-2 unc-52*/+ *lin-31 unc-52* were picked, from which homozygous *smu-2 unc-52* segregants were identified. For *unc-52*(*e444*) and *unc-52*(*e998*), where no suppression or enhancement of the Unc-52 phenotype was observed, the presence of the *smu-2* mutation was confirmed by sequencing. To construct *smu-1*; *smu-2 unc-52* triple mutants, *unc-101*; *smu-2*(*mn416*) *unc-52* hermaphrodites were crossed to *smu-1*; *unc-52* males. Non-Unc-101 Unc-52 progeny, genotype *unc-101* +/+ *smu-1*; *smu-2 unc-52*/ + *unc-52*, were picked. In the next generation, non-Unc-52 progeny that segregated one-fourth Unc-101 progeny (*unc-101*/*smu-1*; *smu-2 unc-52*) were allowed to produce self progeny, and homozygous *smu-1*; *smu-2 unc-52* segregants were identified. The presence of both *smu-1* and *smu-2*(*mn416*) was confirmed by sequencing. To evaluate the extent of Unc-52 suppression, synchronous populations of worms were observed every 12 h throughout development until all worms were gravid adult hermaphrodites. The stage at which approximately 90% of the worms were paralyzed was recorded. For *smu-2* (*mn416*) *unc-52*(*e1421*) worms, we also counted the number of unhatched eggs and hatched larvae 24 h after removal of egg-laying hermaphrodites from a growth plate. *smu-2 unc-52*(*e1421*) animals were also scored for morphology (by differential interference contrast [DIC]microscopy), growth, and movement.

Cloning *smu-2*. Transformation rescue of *smu-2*(*mn416*) was performed by injecting YAC DNA (100 ng/μl) or long-range PCR fragments (20 ng/μl) and the cosmid R1p16 (50 ng/μl), which rescues *unc-36*, into the gonads of *smu-2*(*mn416*) *unc-52*(*ts*); *unc-36* young adult hermaphrodites, as described previously (32). Non-Unc-36 descendants of injected animals grown at 25°C were scored as adults for reappearance of the Unc-52 phenotype. YAC DNA was prepared as described previously (10), and long-range PCR products were made with the Expand long-template PCR system (Boehringer Mannheim). We also tested several DNA samples for *smu-2* rescue in a *mec-8*; *smu-2*(*mn416*); *unc-36* background by scoring for reversal of the suppression by *smu-2* of the dye-filling defect conferred by *mec-8* (28). Sequencing of *smu-2* alleles was done with the Thermosequenase cycle sequencing kit (U.S. Biochemicals) or by the Advanced Genetics Analysis Center (University of Minnesota). A rescuing clone, pAS10, containing all of the *smu-2* coding genomic sequence and 2 kb upstream of the predicted translational start site, was made by cloning the LR16F (CTGTGAT GATGGTTGAAGGTGAC)/LR15R (GACAATGGCTGAAATGATCGATA GTTGG) PCR product into the EcoRV site of pBluescript SK(−) (Stratagene). The PCR product LR16F/LR18R (CACGTTCTTTTTCACGTTCACGGC), which truncates the *smu-2* gene where the *mn610* mutation resides, also rescued *smu-2*. pAS14 was made by removing an NcoI/XhoI fragment from pAS10. pAS19 was created by inserting a NotI *smu-2* genomic fragment from pAS10 into yk563h8, a full-length *smu-2* cDNA. pAS21 was made by cutting and filling in the

HindIII site of pAS19, thereby creating a frameshift mutation at amino acid 45. LR16F/LR15R(*mn610*) and LR16F/LR15R(*mn416*) were made by PCR using 16F and 15R primers with *mn610* and *mn416* mutant genomic DNA as the template. All cloning was done by standard molecular biology techniques (40).

dsRNA interference of *smu-2*. Double-stranded RNA (dsRNA) interference was performed by injection of 1 mg of *smu-2* dsRNA/ml, corresponding to nucleotides (nt) 1041 to 1721 of the *smu-2* transcript. Sense and antisense RNAs were made with a T7/T3 Megascript in vitro transcription kit (Ambion) and purified by phenol-chloroform extraction in accordance with the manufacturer's protocol. Equivalent amounts of RNA were annealed in 3× IM buffer (20 mM KPO_4 [pH 7.5], 3 mM K citrate, 2% polyethylene glycol 6000) at 68°C for 10 min and 37°C for 30 min. Progeny that were laid 24 h after injection were evaluated for embryonic lethality and the Unc-52 phenotype (at 25°C). In control experiments, 3× IM buffer was injected.

RNA isolation. Semisynchronous larval populations were obtained by collecting embryos from bleached hermaphrodites (24) and allowing them to hatch on plates with food for 25 to 26 (L2 population) or 40 h (L4 population) at 20°C. For RNase protection experiments, *unc-52*(*ts*) and *smu-2 unc-52*(*ts*) larvae were grown at 25°C for 30 h to obtain L4 populations. Larvae were washed with M9 buffer (45) and frozen at −80°C. Fifty to 100 μl of concentrated worms was vortexed in 1.6 ml of Trizol (Life Technologies) with glass beads; the supernatant was mixed with 0.32 ml of chloroform, and the RNA was precipitated in 1 volume of isopropanol. RNA pellets were resuspended in 50 to 200 μl of diethyl pyrocarbonate-treated distilled H_2O (dH_2O). RNA samples for reverse transcription-PCR (RT-PCR) were treated with 1 μl of DNase RQ1 per 10 μg of RNA (Promega), extracted with phenol-chloroform, and resuspended in 10 to 15 μl of dH_2O. RNA for *smu-1*::*HA* RT-PCR was obtained from mixed-stage populations and prepared as described above.

RT-PCR. Reverse transcription of 1 to 2 μg of total RNA was performed with Superscript II reverse transcriptase (Life Technologies) in a 20-μl total volume by following the manufacturer's protocol; 60 μl of water was added to the reverse transcription reaction mixture, and 1 μl of this (or a 0.5 or 0.25 dilution) was used for PCR amplification, as described previously (43). PCR was performed with the *unc-52* primers 16F (29) and 18/19R and the *ama-1* primers A3 and B2 (43). Southern blots of PCR products were probed with ^{32}P-end-labeled *unc-52* 16FB and *ama-1* A2 oligonucleotides (43) and quantified with a phosphorimager (Molecular Dynamics) and ImageQuant software (Amersham Pharmacia Biotech). For each cDNA, PCR was performed with increasing cycle numbers (from 16 to 32 cycles) and increasing dilutions (1, 0.5, and 0.25 at 24 or 26 cycles) to evaluate the linearity of the experiments. PCR experiments using *unc-52* primers were repeated with two independent sets of cDNAs from both *smu-2* and wild-type L2 larvae and two independent sets of cDNAs from both *smu-2* and wild-type L4 larvae. *ama-1* primers were included in PCRs with one set of *smu-2* and wild-type L2 cDNAs and one set of *smu-2* and wild-type L4 cDNAs. Three samples which were within the linear range of the PCR were averaged to obtain a ratio of 16-18-19/16-17-18-19 transcripts and a ratio of 16-18-19/*ama-1* transcripts, where appropriate, for each independent experiment. The mean 16-18-19/16-17-18-19 ratios for *smu-2* and for the wild type were calculated from the four independent experiments, and the means were compared statistically with a paired *t* test. RT-PCR of *smu-1*::*HA* was performed with the *smu-1* primers *smu-1*-for (GAAATATCAGGCCCAAGA) and HA-rev (CTCGAGGCACTG AGCAGC) and the *ama-1* primers A3 and B2. *smu-1*::*HA* RT-PCRs were performed within the linear range of amplification.

RNase protection. RNase protection was performed as previously described (43) with 5, 10, and 15 μg of total RNA, 2.5 μl of [^{32}P]CTP (800 Ci/mmol, 20 mCi/ml), and an RPAIII kit (Ambion). The *unc-52* 16-18 RNA probe was generated from pCS168 linearized with HindIII (43) and transcribed with a T7 Maxiscript in vitro transcription kit (Ambion). In addition, a 267-bp *ama-1* probe that protects nt 104 to 371 of the *ama-1* cDNA was included in each experiment. To confirm the sizes of 16-18, 16-17, and 16-19 protected RNAs, sense RNAs corresponding to these RNA species were generated with a T7 Megascript in vitro transcription kit (Ambion) and the appropriate PCR templates. These sense RNAs produced protected bands of the expected sizes when hybridized to the *unc-52* probe. Quantitative data were collected with a phosphorimager as for RT-PCR. The linearity of each RNase protection experiment was evaluated by using multiple concentrations of RNA (5, 10, and 15 μg) in each experiment. A ratio of 16-18/(16-17 plus 16-19) transcripts and of 16-18/*ama-1* transcripts was obtained for each experiment by taking the mean from these three samples. The combined ratios from three experiments performed on two separate sets of RNA isolations that compared *smu-2 unc-52* RNA to *unc-52* RNA gave essentially the same results. Similar data were also obtained when comparing *smu-2* to the wild type.

SMU-2 reporter strains. Plasmid pAS17, which is a *smu-2*::*gfp* reporter that complements *smu-2*(*mn416*), was made by cloning an Eco01019I fragment from the vector pPD118.85 (A. Fire; www.ciwemb.edu) into the Eco01019I site of pAS10 so that all coding sequences remained in frame. The DNA was injected at a concentration of 20 ng/μl with 50 ng of R1p16 DNA/μl into *smu-2*(*mn416*); *unc-36* hermaphrodites and chromosomally integrated, as *mnIs33*, by gamma irradiation (32). The *mnIs33*-bearing stock was outcrossed several times. To evaluate SMU-2::green fluorescent protein (GFP) expression, *smu-2*(*mn416*); *unc-36*; *mnIs33*[*smu-2*::*gfp unc-36*(+)] embryos and larvae were fixed in methanol-acetone as described previously (10) and washed once in phosphate-buffered saline (PBS) containing 0.02 μg of DAPI (4′,6′-diamidino-2-phenylindole)/ml and twice in PBS. With rare exceptions, DAPI fluorescence and GFP autofluorescence were observed in all cells. A *smu-2*::*HA* rescuing construct was made by replacing the natural stop codon of *smu-2* with an XhoI site and inserting a sequence encoding three copies of an hemagglutinin (HA) epitope tag (46) flanked by XhoI sites. Immunofluorescence images of *smu-2*(*mn416*) *unc-52* (*e669su250*); *unc-36*; *mnIs66*[*smu-2*::*HA*; *unc-36*(+)] animals were collected as described below for *smu-1*::*HA*.

Western blots. Western blotting was performed by standard procedures (40). Briefly, adult stage populations of worms were washed with 1 ml of water, and an equal amount of 2× sodium dodecyl sulfate (SDS) loading buffer was added to the worm pellet. The worms were flash-frozen in liquid nitrogen and immediately boiled for 5 min; 40 μl of this lysate was loaded in each lane. Western blots were blocked in blocking buffer (5% condensed nonfat milk, 1× PBS, 0.5%Tween), incubated overnight with the primary antibody, washed three times (5 min each) in 1× PBS–0.5% Tween, incubated for 2 h with the secondary antibody, washed three times (15 min each), and visualized with the ECL detection system (Amersham Pharmacia). The following antibodies were diluted in blocking buffer: rat anti-HA monoclonal antibody (MAb) 3F10 (1:500; Roche), mouse antiactin MAb C4 (1:20,000; ICN Biochemicals), horseradish peroxidase (HRP)-conjugated goat anti-rat (1:5,000; Pierce), and HRP-conjugated goat anti-mouse (1:5,000; Pierce).

Immunofluorescence. Immunofluorescence studies of *smu-1*::*HA* (43) and *smu-2*::*HA* strains were performed on mixed-stage worms as described previously (11) using rat anti-HA MAb 3F10 diluted 1:200 (Roche) and Cy-3-conjugated goat anti-rat diluted 1:1,000 (Jackson Immunoresearch). L1 larvae were also fixed and stained with a methanol-acetone fixation-permeabilization protocol (28).

In vitro coimmunoprecipitation. One microgram of circular plasmid DNA from pAS53 (*smu-2*::*myc*) and pAS59 (*smu-1*::*no tag*) was transcribed and translated in vitro in a 20-μl total volume with the TnT T7 quick-coupled transcription-translation system (Promega) as recommended by the manufacturer, with 1 μl of [^{35}S]methionine (1,000 Ci/mmol at 10 mCi/ml; Amersham Pharmacia) and 1 μl of antimyc MAb 9E10 (Santa Cruz Biotechnology). To the in vitro-translated proteins, 30 μl of a 50% slurry of protein G-agarose beads (Sigma) and immunoprecipitation buffer E (20% glycerol, 20 mM HEPES [pH 7.9], 0.125 mM EDTA, 100 mM KCl, 0.1% NP-40, 0.5 mM dithiothreitol, and mini-EDTA-free protease inhibitor cocktail [Roche]) was added to make a final volume of 100 μl, and the mixture was incubated at 4°C for 1 h. The beads were then precipitated, washed three times in 200 μl of buffer E, resuspended in 1× SDS loading buffer, and boiled, and proteins were electrophoresed through an SDS–8% polyacrylamide gel. In all constructs, the vectors T7plinkTag and T7plink (9) were used for production of in vitro-translated proteins with and without the myc tag, respectively. pAS53 (*smu-2*::*myc*), pAS63 (*smu-2*::*no tag*), pAS59 (*smu-1*::*no tag*), pAS57 (*smu-1*::*myc*), and pAS55 (*mec-8*::*myc*) all contain the full coding regions for their respective genes. Control plasmids pDZ45 and pDZ46 (partial *tra-1* clones in T7plink and T7plinkTag, which encode the N terminus through the DNA binding domain of TRA-1), were obtained from D. Zarkower, and plasmid pHG35 (full-length *tim-1* clone in T7plink) was obtained from H. Gardner.

In vivo coimmunoprecipitation. To obtain a strain containing both *smu-2*::*HA* and *smu-1*::*gfp*, animals of genotype *smu-2*(*mn416*) *unc-52*(*ts*); *unc-36*; *mnIs66* [*smu-2*::*HA unc-36*(+)] (strain SP2693) were crossed to *smu-1*; *unc-36*; *mnIs31* [*smu-1*::*gfp*; *unc-36*(+)] animals and descendants homozygous for both *mnIs66* and *mnIs31* were identified by antibody staining and fluorescence microscopy. To obtain a strain containing both *smu-2*::*HA* and *sur-5*::*gfp*, strain SP2693 was injected with 50 ng of *sur-5*::*gfp*/μl (50) and 100 ng of pRF4/μl (33). A resulting strain, genotype *smu-2*(*mn416*) *unc-52*(*ts*); *unc-36*; *mnIs66*[*smu-2*::*HA unc-36*(+)]; *mnEx161*[*sur-5*::*gfp*; *rol-6*(*d*)], which transmitted *mnEx161* to approximately two-thirds of its progeny, was used for coimmunoprecipitation. To prepare embryo lysates, worms were grown for two generations. The embryos from bleached hermaphrodites (24) were washed three times in M9 buffer and once in HB buffer (50 mM HEPES, 1 mM EDTA, 1 mM EGTA, 100 mM NaCl, 100 mM

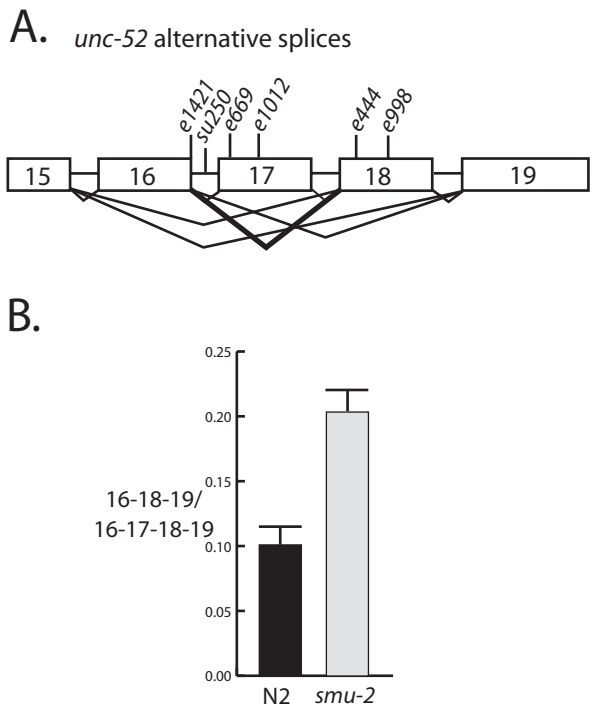

FIG. 1. RT-PCR analysis of *unc-52* transcripts in *smu-2* mutants. (A) Depiction of the alternatively spliced region of *unc-52*. Boxes, exons 15 to 19; horizontal lines, introns. The locations of *unc-52* viable mutations used in this study are indicated. The heavy lines from exon 16 to exon 18 indicate the alternatively spliced transcript that shows increased abundance in *smu-2* mutants. (B) Results from four independent RT-PCR experiments performed on *smu-2*(*mn416*) and wild-type (N2) larvae. The mean ratios of 16-18-19/16-17-18-19 *unc-52* transcripts were 0.100 ± 0.015 in wild-type (N2) larvae and 0.204 ± 0.018 in *smu-2* larvae; these values were found to be significantly different in a paired *t* test ($P = 0.025$). These data indicate that there is approximately a twofold increase in the 16-18-19 transcript in *smu-2* mutants.

KCl, 1 mM dithiothreitol, 4 mM NaF, 1 mM phenylmethylsulfonyl fluoride, 5% glycerol, 0.3 μg of aprotinin/ml, 0.5 μg of pepstatin/ml, and mini-EDTA free protease inhibitor cocktail [Roche]) and were resuspended in 400 μl of HB buffer. Embryos were sonicated, centrifuged at 16,000 × *g* for 10 min (4°C) to remove cellular debris, and then cleared by centrifugation for 2 min at 16,000 × *g*. Approximately 900 μg of total worm protein was preincubated in 25 μl of 50% protein G-agarose beads (Sigma) plus 2 μg of mouse immunoglobulin G (Sigma) for 4 h at 4°C. The supernatants were then incubated with 5 μl of mouse 3E6 anti-GFP (QBiogene) antibody overnight at 4°C. Twenty-five microliters of protein G-agarose beads was added, incubated for 1 h, precipitated, washed three times in 500 μl of HB buffer, and resuspended in SDS loading buffer. Proteins were electrophoresed through an SDS–8% polyacrylamide gel, and Western blots were prepared as described above with rat anti-HA MAb 3F10 (1:1,000) or a chicken anti-GFP antibody (1:10,000) (Chemicon) with HRP-conjugated donkey anti-chicken (1:5,000; Jackson Immunoresearch). Western blots for coimmunoprecipitation experiments were visualized with SuperSignal ELISA Femto maximum-sensitivity substrate (Pierce).

RESULTS

Mutations in *smu-2* and *smu-1* exhibit identical patterns of interaction with different *unc-52* mutations. It was shown previously (28) that *smu-2* mutations fully suppress the adult onset paralysis conferred by the temperature-sensitive *unc-52* allele *e669su250*. This allele contains the *e669* mutation, a premature stop in exon 17, and the point mutation *su250* in intron 16 (Fig. 1A), which acts as a partial suppressor of *e669* (30, 37). Whereas *e669su250* animals become paralyzed as adults when grown at 25°C, *smu-2 unc-52*(*e669su250*) animals never become paralyzed. Mutations in *smu-2* also weakly suppress the *e669* mutation by itself: *smu-2 unc-52*(*e669*) animals became paralyzed about 24 h later than do *unc-52*(*e669*) animals (28). We tested the ability of *smu-2* mutations to suppress additional *unc-52* viable alleles (Table 1). We found that *smu-2* mutations delayed the onset of paralysis conferred by the *unc-52*(*e1012*) mutation, another exon 17 nonsense mutation (37), by about 24 h. But *smu-2* mutations did not suppress either the *unc-52* (*e444*) or *unc-52*(*e998*) mutation, which are nonsense mutations in exon 18 (37). We also found that mutation in *smu-2* did not delay the adult onset paralysis conferred by the *unc-52* (*e1421*) mutation, which is a single base pair change in the 5′ splice site of intron 16 (37). On the contrary, we found that two-thirds of the *smu-2 unc-52*(*e1421*) embryos exhibited elongation defects similar to those observed in *smu-1*; *unc-52* (*e1421*) embryos (43); 37% of *smu-2 unc-52*(*e1421*) progeny arrested during embryogenesis, and another 29% hatched as abnormal larvae (Table 1). DIC microscopy showed that arrested embryos and hatched abnormal larvae had bulges and constrictions along the length of their bodies. The abnormal larvae grew more slowly and were less mobile than their siblings of the same age. The remaining 34% of *smu-2 unc-52* (*e1421*) progeny were normal in appearance and moved well until the adult stage, when Unc-52 paralysis occurs. The lethality of *smu-2 unc-52*(*e1421*) embryos resembles, but is less severe than, the lethality observed in *unc-52* null mutants, which occurs at the twofold stage of embryogenesis (49). Thus the effect of *smu-2* mutation on *unc-52*(*e1421*) can be thought of as an enhancement of the *unc-52* reduced-function phenotype.

smu-1 has been characterized both genetically and molecularly (43). Mutations in *smu-1* interact with the *unc-52* viable alleles identically to mutations in *smu-2*: they suppress the *unc-52* alleles *e669*, *e1012*, and *e669su250*; they fail to suppress

TABLE 1. Genetic interactions among *smu-2, smu-1*, and *unc-52* mutations

Genotype[a]	Developmental stage at onset of paralysis
unc-52(*e669su250*)	Adult
unc-52(*e669*)	Late L4
unc-52(*e1012*)	Late L4
unc-52(*e444*)	Early L4
unc-52(*e998*)	Early L4
unc-52(*e1421*)	Adult
smu-2(*mn416*) *unc-52*(*e669su250*)	None
smu-2(*mn416*) *unc-52*(*e669*)	Adult
smu-2(*mn416*) *unc-52*(*e1012*)	Adult
smu-2(*mn416*) *unc-52*(*e444*)	Early L4
smu-2(*mn416*) *unc-52*(*e998*)	Early L4
smu-2(*mn416*) *unc-52*(*e1421*)	Embryo; adult[b]
smu-1; *unc-52*(*e669*)	Adult
smu-1; *unc-52*(*e1012*)	Adult
smu-1; *smu-2*(*mn416*) *unc-52*(*e669*)	Adult
smu-1; *smu-2*(*mn416*) *unc-52*(*e1012*)	Adult

[a] Strains containing *e669su250* were grown at 25°C. All others were grown at 20°C.

[b] Thirty-seven percent of *smu-2 unc-52*(*e1421*) double mutants die as embryos, while 29% of the remaining larvae that hatch show abnormalities consistent with muscle defects. Those embryos that survive to adulthood with no or few abnormalities become uncoordinated at the adult stage in the same manner as *unc-52*(*e1421*) mutants.

e444 and *e998*; and they enhance *e1421*. Mutations in *smu-1* and *smu-2* suppress the mechanosensory and chemosensory defects conferred by *mec-8* mutations and the cold-sensitive partially penetrant embryonic lethality conferred by null *mec-8* alleles (28). The similar phenotypes of *smu-1* and *smu-2* mutants suggest that these genes act in the same pathway. To address this question genetically, we constructed *smu-1*(*null*); *smu-2*(*mn416*) *unc-52*(*e669* or *e1012*) triple mutants and evaluated their paralysis phenotypes. Suppression of *unc-52* by *smu-1*; *smu-2* mutations together appeared to be identical to suppression by either *smu-1* or *smu-2* mutations alone (Table 1). Furthermore, the *smu-1*; *smu-2* double-mutant strains were no less healthy than either *smu-1* or *smu-2* single-mutant strains. These results are consistent with *smu-1* and *smu-2* acting in the same pathway.

Mutations in *smu-2* affect the accumulation of alternatively spliced *unc-52* transcripts. Exons 16, 17, and 18 of *unc-52* each encode a single immunoglobulin or NCAM repeat (38). Alternative splicing of the *unc-52* transcript in this region leads to the synthesis of different protein isoforms with various numbers of these repeats, reflecting various patterns of exon skipping (Fig. 1A). The genetic interactions between the *smu-2* and the *unc-52* mutations that we have observed suggest that the *smu-2* mutations suppress *unc-52* nonsense mutations in exon 17 but not exon 18 by increasing the production of *unc-52* transcripts that skip exon 17 but not exon 18. To test this hypothesis, we evaluated the levels of *unc-52* transcripts in *smu-2* mutants by semiquantitative RT-PCR and RNase protection. For RT-PCR analysis we measured the level of the *unc-52* 16-18-19 transcript with respect to the level of the *unc-52* 16-17-18-19 transcript, which is the major larval *unc-52* transcript, and to the level of the *ama-1* transcript. The abundance of the *ama-1* transcript, which encodes the large subunit of RNA polymerase, is unchanged throughout development (18, 19) and serves as an internal control. To ensure that we were quantifying PCR products that were within the linear range of amplification, we analyzed the PCRs at increasing cycle numbers (16 cycles through 32 cycles) and at increasing dilutions of cDNA template (1, 0.5, and 0.25). Southern blots for each PCR experiment were probed with specific *unc-52* or *ama-1* probes and quantified by densitometry and ImageQuant software. Four independent RT-PCR experiments using RNA preparations from L2 and L4 larvae compared the abundance of *unc-52* 16-18-19 transcripts to that of 16-17-18-19 transcripts in *smu-2* and wild-type animals, with essentially identical results. Combined data for all four experiments showed a statistically significant difference in the ratio of 16-18-19 transcripts to 16-17-18-19 transcripts in *smu-2* mutants compared to the wild type, indicating about a twofold increase in the abundance of the *unc-52* 16-18-19 isoform in *smu-2* mutants (Fig. 1B). In two experiments we measured the ratio of 16-18-19 transcripts to *ama-1* transcripts, which also increased by about 1.7-fold in *smu-2* mutants compared to the wild type (data not shown). By contrast, the ratio of 16-17-18-19 transcripts to *ama-1* transcripts in *smu-2* mutants did not change (data not shown). We also did not detect changes in any of the other *unc-52* transcripts, such as 16-17-19 and 15-18-19, in *smu-2* mutants (data not shown).

We performed RNase protection experiments to confirm the RT-PCR results. The *unc-52* RNA probe contained 108 nt from pBluescript SK(−), the last 219 nt of exon 16, and the first 11 nt of exon 18 (Fig. 2A). 16-18-19 transcripts protected 230 nt of the probe, whereas 16-17-18-19 and 16-19 transcripts should protect 219 and 220 nt of the probe, respectively. Reconstruction experiments showed that the 219- and 220-nt bands did not reliably distinguish 16-17-18-19 transcripts from 16-19 transcripts, and so they were grouped together for analysis. A probe protected by *ama-1* transcripts was also used as an internal control. Combined data from three independent RNA preparations showed a statistically significant increase in the level of 16-18-protected fragments in *smu-2 unc-52*(*ts*) mutants compared to *unc-52*(*ts*) animals when animals were grown at 25°C (Fig. 2B). An approximately twofold increase in the ratio of the 230-nt fragment (16-18) to the 219- to 220-nt

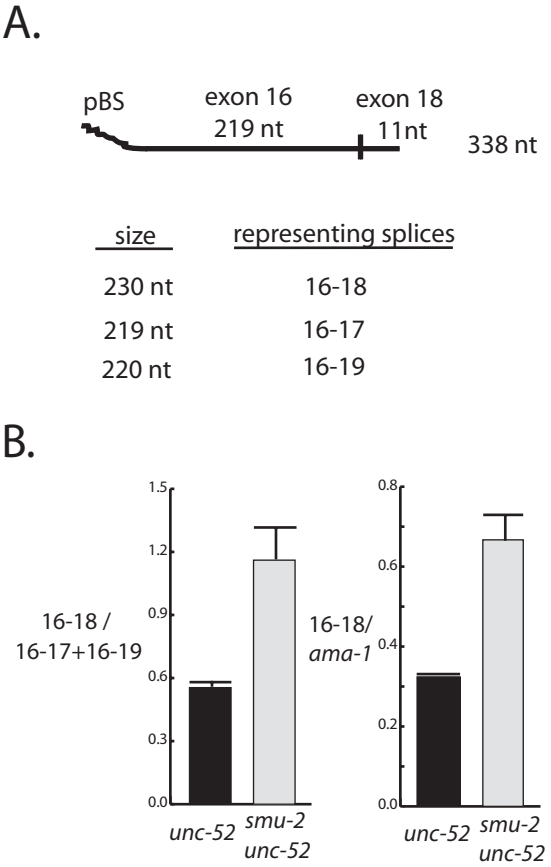

FIG. 2. RNase protection analysis of *unc-52* transcripts in *smu-2* mutants. (A) Depiction of the *unc-52* probe used for RNase protection experiments. The complete probe transcribed from the T7 promoter and including vector sequences is 338 nt long and contains 219 nt of exon 16 and 11 nt of exon 18. Probe lengths protected by different splice forms are indicated. (B) Data from three independent RNase protection experiments from *unc-52* and *smu-2 unc-52* larval RNA. The data from the 219- and 220-nt protected fragments, representing 16-17 and 16-19 splice forms, were grouped together because the fragments do not reliably distinguish these transcripts. The mean ratios for 16-18/(16-17 plus 16-19) transcripts was 0.545 ± 0.032 for *unc-52* larvae and were 1.157 ± 0.156 for *smu-2 unc-52* larvae; these values were found to be significantly different in a paired *t* test ($P = 0.041$). Mean ratios for 16-18/*ama-1* transcripts were 0.323 ± 0.0002 for *unc-52* animals and 0.667 ± 0.065 for *smu-2 unc-52* animals; these values were also found to be significantly different in a paired *t* test ($P = 0.034$). These data indicate that there is about a twofold increase in the abundance of the 16-18 splice form in *smu-2* mutants.

bands (16-17 plus 16-19) or to the *ama-1* band was observed in *smu-2 unc-52*(*ts*) animals compared to *unc-52*(*ts*) animals. As expected, no change was observed for the 219- to 220-nt band compared to the *ama-1* band (data not shown). We repeated the experiment with N2 and *smu-2* L4 RNA to eliminate any differential effects of the *unc-52* mutation and found a similar increase in the 16-18 transcripts in *smu-2* mutants (data not shown). We conclude from these and our RT-PCR analyses that the levels of 16-18-19 transcripts increase about twofold in *smu-2* mutants, as has been observed in *smu-1* mutants (43).

Molecular identification and characterization of *smu-2*. We mapped *smu-2* about 1 centimorgan to the left of the cloned gene *lin-31*. To refine the position of *smu-2* on the physical map, we identified five sequence dimorphisms between strains N2 and RC301 in the *smu-2* region. We then analyzed 26 crossovers between *smu-2* and *lin-31* in which the *smu-2 lin-31* chromosome was derived from N2 and the recombining chromosome carried the RC301 sequence. We scored each crossover with respect to its inheritance of sequence dimorphisms (see Materials and Methods). The results placed *smu-2* between dimorphisms *mnP5* and *mnP4* on the physical map (Fig. 3A). Using DNA from this region, we identified *smu-2* by transformation rescue. Rescue was observed as the (unsuppressed) appearance of the Unc-52 phenotype at 25°C in *smu-2*(*mn416*) *unc-52*(*ts*) animals injected with candidate DNA. We were able to rescue *smu-2* with the YAC Y37F3, the long-range PCR product LR13, and the long-range PCR product 16F/15R, which contains the single predicted gene Y49F6B.4 (Fig. 3B). This gene lies 18 kb to the right of *mnP5* and 17.9 kb to the left of *mnP4*. To show that Y49F6B.4 is *smu-2*, we replaced genomic sequence after the first predicted intron with a full-length cDNA (yk563h8) corresponding to Y49F6B.4. This construct, which contains only 2 kb of genomic sequence upstream of the predicted translational start codon, rescued *smu-2* (Fig. 3C). A frameshift mutation introduced in this construct at predicted codon 45 abolished rescue. We sequenced two alleles of *smu-2* and found molecular lesions in the Y49F6B.4 gene (Fig. 4). *mn416* has a 3′ splice site mutation in intron 1 (AG/AAA to AA/AAA). *mn610* has a single base pair deletion in exon 6 that results in a frameshift after amino acid 407. A third allele, *mn611*, has a rearrangement, identified by Southern blotting and PCR (data not shown), in the last quarter of the *smu-2* coding sequence. The analysis of several expressed sequence tags in sequence databases and our observation of a single band on Northern blots (data not shown) suggest that *smu-2* encodes a single protein. Sequencing of yk563h8 confirmed the predicted intron-exon boundaries. Our experiments involving 5′ rapid amplification of cDNA ends showed that the transcription start site is located 77 bases upstream of the AUG start codon (position 160113 of Y49F6B) and that the transcripts are not *trans*-spliced to SL1 or SL2 (data not shown).

Database searches revealed that SMU-2 is a highly conserved protein with homologs in vertebrates, invertebrates such as *D. melanogaster*, and plants such as *Arabidopsis thaliana*. The N terminus of a *Schizosaccharomyces pombe* protein also shows limited similarity to SMU-2. SMU-2 is 39.8% identical to a human protein that has been isolated by two groups from purified human spliceosomes and identified by mass spectrometry (35, 52). The human protein has been called IK factor (22, 35) and, more recently, RED (1, 52). RED has been shown to localize to the nucleus and to be present in all tissue types (1). RED was named after a domain rich in arginine (R), aspartic acid (E), and glutamic acid (D) residues. In the alignment of SMU-2 with its human, *Drosophila*, and *Arabidopsis* homologs, it is apparent that the RED domain itself is not highly conserved (Fig. 4). SMU-2 contains a series of RD repeats in this region, but it also contains several serine residues and an extensive region that is rich in aspartic acid and lysine residues (an EK domain). Surprisingly, the *Drosophila* and *Arabidopsis* homologs do not contain any semblance of a RED domain. Secondary structure predictions and examination of amino acid charge distribution also fail to find conserved features in this region for all four proteins. Although SMU-2 is predicted to contain a coiled-coil domain in this region, the others are not.

The *smu-2* null phenotype. Our molecular analysis of three *smu-2* mutations revealed that none is a candidate null mutation. Indeed, we have shown that PCR products generated from either *mn416* or *mn610* DNA can rescue the *smu-2* mutant phenotype (Fig. 3C), presumably owing to overexpression by the multicopy arrays that are generated from the injected DNA (32). For *mn416*, which has a 3′ splice site mutation, splicing to exon 2 may sometimes occur, and, for *mn610*, which has a frameshift mutation affecting the last one-third of the protein, overexpression of the truncated protein may rescue *smu-2*. Phenotypically, all three *smu-2* mutants appear to be nearly wild type, although they, much like *smu-1* mutants, have a tendency to coil their bodies and have slightly reduced brood sizes compared to N2 animals. We have determined that *smu-2* (*mn416*)/*ccDf11* animals, in which *ccDf11* deletes *smu-2*, mimic *smu-2*(*mn416*) homozygotes phenotypically, both with respect to their viability and ability to suppress *unc-52*(*ts*), suggesting that the *smu-2* null phenotype is viable. To investigate this point further, we performed dsRNA interference on both *unc-52* mutants and *smu-2*(*mn416*) mutants using *smu-2* dsRNA. *smu-2* RNA interference (RNAi) suppressed *unc-52*(*ts*) very efficiently: 99% of the progeny of injected *unc-52*(*ts*) animals were suppressed (Table 2). To ensure that we were decreasing the levels of *smu-2* mRNA, we injected a strain that contained a rescuing *smu-2*::*gfp* reporter construct (pAS17) and observed that all GFP fluorescence was gone in embryos from injected animals (data not shown). In all of our injections of wild-type, *unc-52*, or *smu-2(mn416)* animals with *smu-2* dsRNA, we never observed any embryonic lethality above that seen in control animals (Table 2) or any other obvious mutant phenotype.

Localization and expression pattern of SMU-2. We made a rescuing construct, pAS17, which produces a fusion protein in which GFP is inserted in the last quarter of the SMU-2 protein (Fig. 3C and 4). We found that SMU-2::GFP is a nuclear protein (Fig. 5). SMU-2::GFP was observed at all stages of development including early embryogenesis and in oocytes (Fig. 5). To show that SMU-2 is ubiquitously expressed, we costained embryos and larvae carrying the integrated *smu-2*::*gfp* array with the DNA stain DAPI and observed SMU-2::GFP in essentially every cell that was stained by DAPI (Fig. 5D and E). Unlike most transgenes in *C. elegans*, the *smu-2*::*gfp* transgene was expressed in the germ line (Fig. 5F and G). To confirm this result with another SMU-2-expressing transgene, we constructed a rescuing transgene that placed a HA tag at the very end of the protein. This construct also led to nuclear expres-

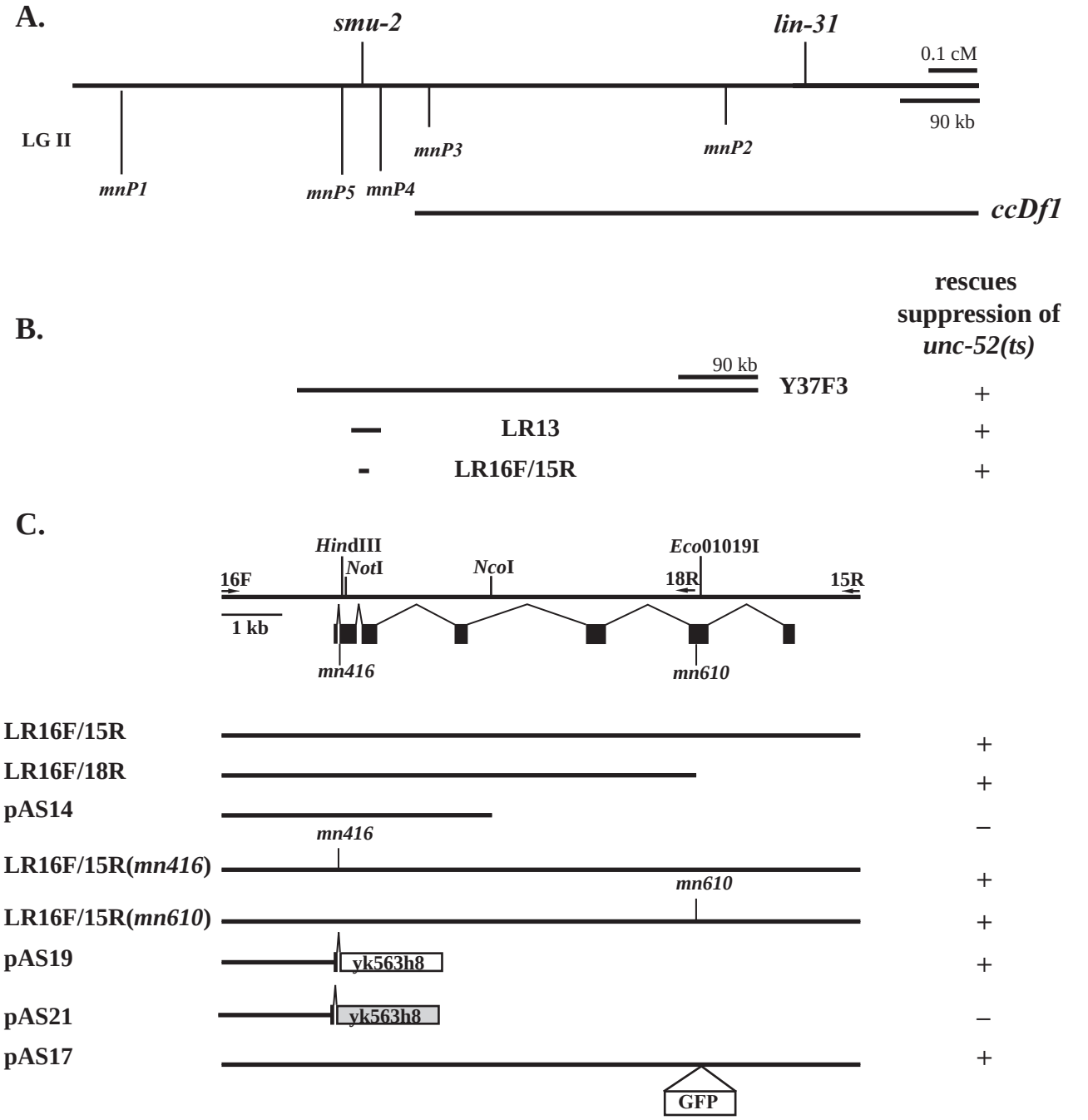

FIG. 3. Mapping and cloning *smu-2*. The scales in panels A and B are identical. (A) Genetic map position of *smu-2* with respect to the *lin-31* gene and DNA sequence dimorphisms between strains N2 and RC301, which were used in mapping. The left end point of *ccDf1*, representing a deficiency that deletes *lin-31* and complements *smu-2*, was mapped between dimorphisms *mnP3* and *mnP4*. (B and C) Transformation rescue data for *smu-2* with YAC DNA and long-range PCR products. + indicates that at least one line that rescued *smu-2*, as assayed by reversal of *unc-52* suppression, was obtained; − indicates that several lines that did not rescue *smu-2* were obtained. (C) The exon-intron structure of *smu-2* is indicated below the restriction map. Arrows, locations of primers used to generate long-range PCR products. Eco01019I, NotI, and HindIII restriction sites used to construct pAS17, pAS19, and pAS21, respectively, are indicated. yk563h8 is a full-length *smu-2* cDNA. pAS21 has a frameshift mutation introduced at the HindIII site (light gray box). The placement of the GFP gene for plasmid pAS17 is shown. *smu-2*(*mn416*) has a point mutation located at the 3′ splice site of intron 1. *smu-2*(*mn610*) has a single base pair deletion in the middle of exon 6. LR16F/15R(*mn416*) and LR16F/15R(*mn610*) are PCR products that were generated from genomic DNA made from the respective *smu-2* mutants.

sion in all cells, including the germ line (data not shown). We occasionally observed that SMU-2::GFP localized to a subnuclear compartment that we believe is the nucleolus because of its morphology and its increased size in *ncl-1* mutants, which have enlarged nucleoli. However, nucleolar localization was dependent on the health of the animal. Animals suffering from prolonged exposure to sodium azide showed a dramatic increase in nucleolar localization. We rarely observed nucleolar

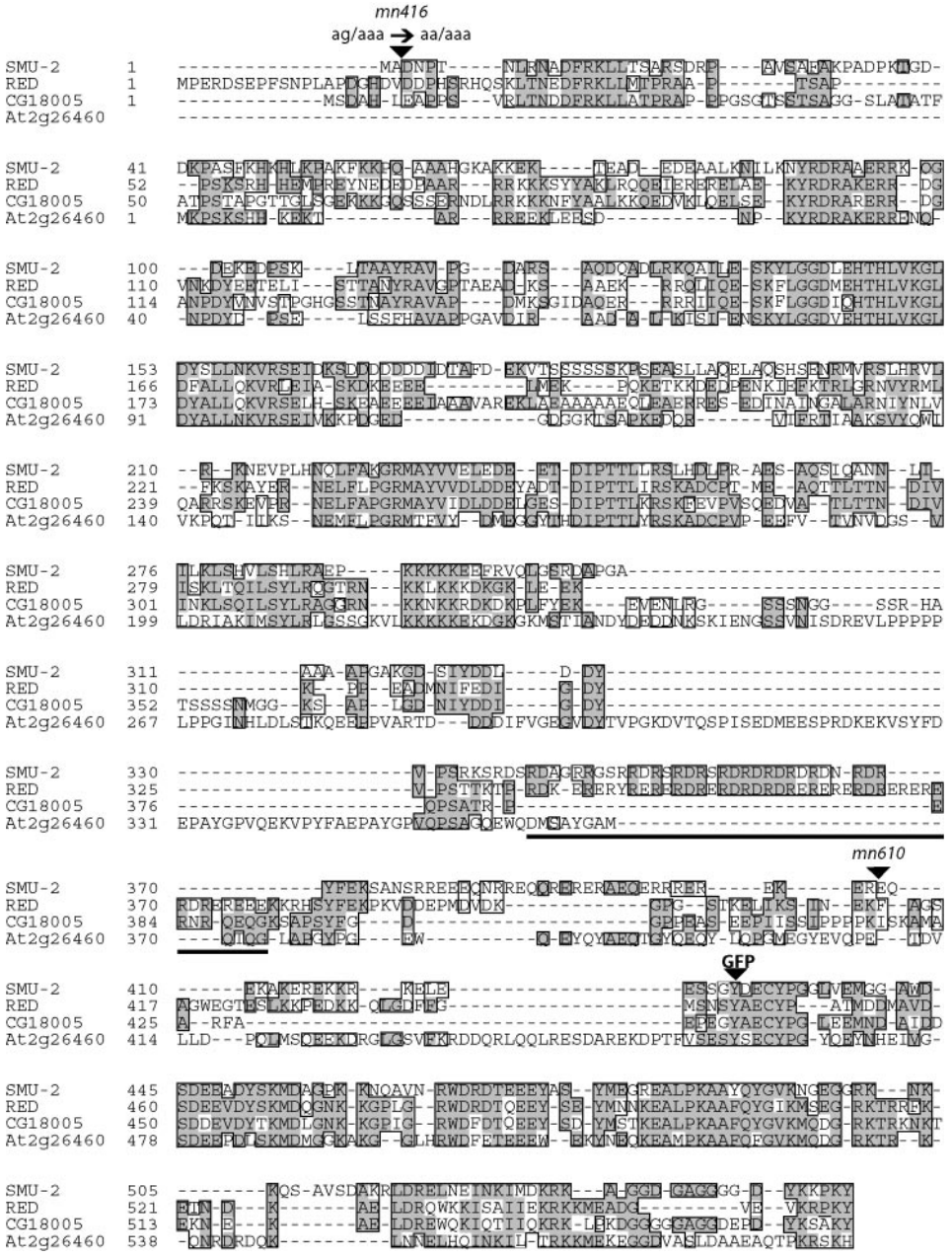

FIG. 4. Alignment of SMU-2 and its homologs. The alignment was adapted from individual pairwise alignments made with the ClustalW program. Similar residues are boxed; identical residues in two or more homologs are shaded. A complete cDNA of the *Drosophila* homolog, CG18005, was sequenced by us. A cDNA corresponding to the *Arabidopsis* homolog, At2g26460, was sequenced by The Institute for Genomic Research. The RED domain of human RED is underlined. The positions of the *mn416* and *mn610* mutations and the insertion site for GFP are indicated.

localization of SMU-2::HA. We suppose that SMU-2 is not normally localized to the nucleolus. We did not observe any other consistent pattern of subnuclear localization.

***smu-2* mutation affects the accumulation of SMU-1.** When either integrated array *smu-1*::*gfp* or *smu-1*::*HA* (43) was present in a homozygous *smu-2*(*mn416*) background, the expression of the corresponding SMU-1 fusion protein was substantially reduced (Fig. 6). For each *smu-1* transgene, limited nuclear expression in a few anterior neurons and hypodermal nuclei in the *smu-2* animals was still observed (Fig. 6A). We analyzed the abundance of SMU-1::HA by Western blotting and saw

TABLE 2. *smu-2* RNAi of *unc-52* and *smu-2* mutant strains

Genotype	% of progeny of injected animals with phenotype:	
	Embryonic lethality[b]	Non-Unc-52
unc-52(*e669su250*)[a]	4.2 (17/408)	1.5 (6/391)
smu-2(*RNAi*) *unc-52*(*e669su250*)	2.2 (10/453)	99.1 (439/443)
smu-2(*mn416*)[a]	2.9 (11/376)	Not applicable
smu-2(*RNAi mn416*)	3.8 (20/530)	Not applicable

[a] Injected with 3× IM buffer.
[b] Numbers in parentheses are ratios of the numbers of embryos with the phenotype to the total numbers of embryos scored from injected hermaphrodites.

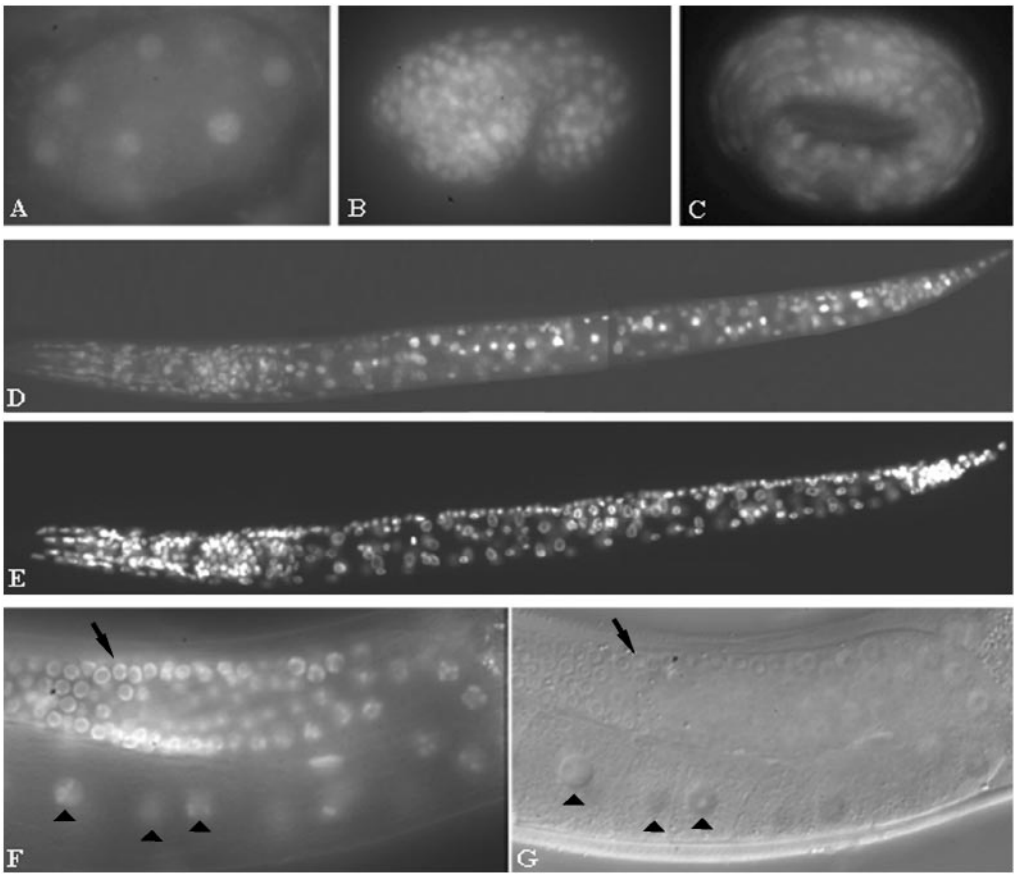

FIG. 5. *smu-2*::*gfp* expression patterns. (A to D) SMU-2::GFP is nuclear and ubiquitously expressed throughout development. (A) A 10-cell embryo. (B) Comma-stage embryo. (C) Threefold-stage embryo. (D) L1 larva. (E) DAPI staining of the nuclei in larva of panel D. (F and G) SMU-2::GFP is expressed in the germ line and oocytes. (F) A portion of the gonad in a young adult worm with nuclear expression in the germ line (arrow) and oocytes (arrowheads). (G) DIC image of the worm in panel F.

that the major SMU-1::HA protein, migrating at 78.5 kDa, was significantly reduced in *smu-2* animals (Fig. 6B). To rule out the possibility that *smu-2* regulates *smu-1* transcription or transcript stability, we performed RT-PCR on these strains to measure *smu-1*::*HA* transcript levels. We observed no changes in *smu-2* mutants compared to *smu-2*(+) animals (Fig. 6C). We suggest that the wild-type SMU-2 protein is required to prevent SMU-1 degradation. SMU-1 seems not to be required for SMU-2 stability, however, because we did not observe any change in *smu-2*::*gfp* expression in *smu-1* mutants (data not shown).

Evidence that SMU-2 and SMU-1 directly interact. Genetic evidence suggests that *smu-2* and *smu-1* act together; both proteins are ubiquitously expressed in the nucleus, and SMU-1 accumulation depends on SMU-2. We therefore sought evidence of a SMU-1/SMU-2 physical interaction by performing in vitro and in vivo coimmunoprecipitation experiments.

SMU-2::MYC tagged protein and untagged SMU-1 were labeled with [^{35}S]methionine by coupled in vitro transcription and translation and immunoprecipitated with an antimyc antibody. As shown in Fig. 7, we consistently observed that SMU-2::MYC was able to coimmunoprecipitate SMU-1. SMU-1 was not coimmunoprecipitated by other nuclear proteins, such as MEC-8 and TRA-1, the latter a transcription factor that regulates *C. elegans* sex determination (14, 51) (Fig. 7A). In similar experiments we saw that SMU-2::MYC was unable to coimmunoprecipitate other nuclear proteins, such as untagged TRA-1 and untagged TIM-1, a protein that regulates chromosome cohesion (8) (data not shown).

To show that SMU-1 and SMU-2 interact in vivo, we performed coimmunoprecipitation experiments on worms expressing tagged SMU-1 and SMU-2 proteins. Embryo lysates were prepared from strains containing *smu-2*::*HA* alone, both *smu-2*::*HA* and *smu-1*::*gfp*, and both *smu-2*::*HA* and *sur-5*::*gfp*. Lysates were immunoprecipitated with an anti-GFP antibody, and immunoprecipitates were analyzed for SMU-2::HA. SUR-5::GFP is a nuclear protein of unknown function (50) and served as a control to show that SMU-2 does not interact nonspecifically with nuclear proteins or with GFP. We found that SMU-1::GFP and SMU-2::HA consistently coimmunoprecipitated but that SUR-5::GFP and SMU-2::HA did not (Fig. 7B).

DISCUSSION

***smu-2* regulates the alternative splicing of *unc-52* transcripts.** We have shown that recessive mutations in *smu-2* lead to enhanced accumulation of *unc-52* transcripts in which exon 17, but not exon 18, has been skipped. Loss-of-function muta-

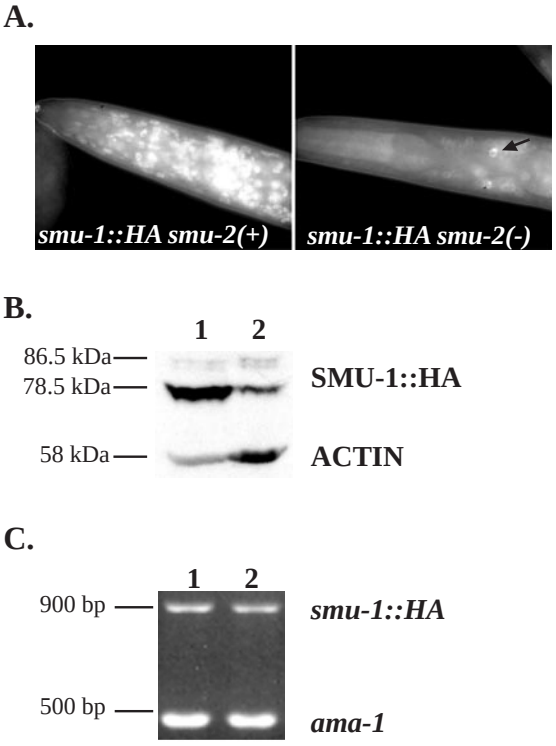

FIG. 6. Effect of *smu-2* mutation on expression of *smu-1*::*HA*. (A) Anti-HA immunofluorescence of SMU-1::HA in *smu-2*(+) and *smu-2*(*mn416*) genetic backgrounds. HA staining is dramatically reduced in *smu-2* mutants, although staining is observed in some head neurons (arrow). (B) Western analysis of SMU-1::HA in *smu-2*(+) (lane 1) and *smu-2*(*mn416*) animals (lane 2). The major SMU-1::HA protein migrating at 78.5 kDa is markedly reduced in *smu-2* mutants. Both the 78.5- and 86.5-kDa bands are specific to the *smu-1*::*HA* transgene since they do not appear in N2 animals (not shown). An antiactin antibody was used to monitor overall protein levels. (C) RT-PCR analysis of *smu-1*::*HA* transcripts in *smu-2*(+) (lane 1) and *smu-2*(*mn416*) (lane 2) animals. *ama-1* was used as an internal control.

tions in *smu-1* have the same consequence (43). It was concluded for *smu-1* that this accumulation is due to enhanced skipping of exon 17 during splicing rather than to differential effects on mRNA stability (43). The earlier arguments, which need not be repeated here, also apply to *smu-2* and are consistent with both our molecular identification of SMU-2 as a homolog of a human spliceosome-associated protein and the recent identification (52) of a human spliceosome-associated protein with 62% amino acid identity to SMU-1.

The enhanced formation of *unc-52* transcripts that skip exon 17 but not exon 18 supports the idea that *smu-2* mutations suppress the late-onset paralysis conferred by nonsense mutations in exon 17 but not exon 18 by increasing the abundance of functional UNC-52 protein in the extracellular matrix between body wall muscle and hypodermis, where it is needed to help anchor the muscle to the hypodermis and cuticle (16, 49). As animals increase in size during larval and early-adult stages, muscle anchorages must be added to prevent the tearing away of muscle that leads to paralysis in *unc-52*(*viable*) mutants (34, 37). It is not surprising that the suppression of *unc-52*(*e669*) and *unc-52*(*e1012*) is only partial, because the effect of *smu-2* mutations on splicing is fairly small, a twofold increase in 16-18 transcripts. The complete suppression of *unc-52*(*e669su250*) at the restrictive temperature of 25°C is also not surprising because the *su250* mutation, a single base pair change in the middle of intron 16 (37), promotes an increase in the accumulation of 16-18 transcripts even at the restrictive temperature (43).

A somewhat different mechanism is required to explain the interaction that we have seen between a *smu-2* loss-of-function mutation and the *unc-52*(*e1421*) mutation, a 5′ splice site mutation in intron 16. The double mutant exhibits a partially penetrant embryonic lethality that is not seen with either single mutant but which is similar (albeit milder) to the phenotype produced by null *unc-52* alleles. The animals that survive embryogenesis unscathed suffer from late-onset paralysis at the

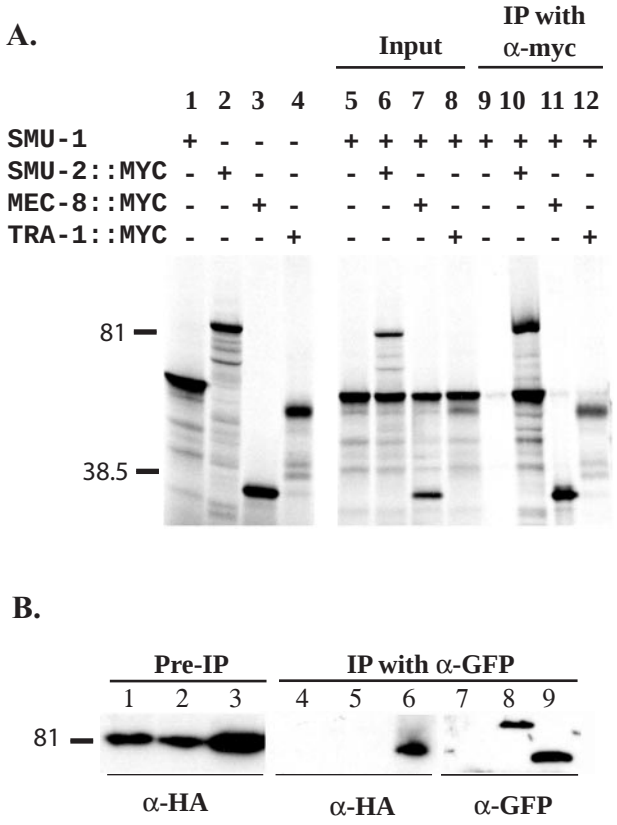

FIG. 7. In vitro and in vivo coimmunoprecipitation of SMU-1 and SMU-2. (A) SMU-1 was transcribed and translated in vitro with either SMU-2::MYC, TRA-1::MYC, or MEC-8::MYC by using [^{35}S]methionine, and the reaction mixture was immunoprecipitated with an antimyc MAb. Proteins were separated by SDS-polyacrylamide gel electrophoresis. Lanes 1 to 4, translation of SMU-1, SMU-2::MYC, MEC-8::MYC, and TRA-1::MYC, respectively; lanes 5 to 8, 1/10 of the input from each total reaction volume; lanes 9 to 12, proteins immunoprecipitated by the antimyc antibody. Labeled proteins were visualized by autoradiography. (B) Protein lysates were made from embryos containing *smu-2*::*HA* (lanes 1, 4, and 7), both *smu-2*::*HA* and *sur-5*::*gfp* (lanes 2, 5, and 8), and both *smu-2*::*HA* and *smu-1*::*gfp* (lanes 3, 6, and 9). Western blots of proteins separated by SDS-polyacrylamide gel electrophoresis were prepared. Lanes 1 to 3, 1/40 of the total protein lysate before coimmunoprecipitation; lanes 4 to 9, 1/2 of the total proteins that were immunoprecipitated with anti-GFP MAb 3E6. Lanes 1 to 6 were probed with the anti-HA MAb, and lanes 7 to 9 were probed with chicken anti-GFP.

same time that single-mutant *unc-52*(*e1421*) animals do. We presume that the *e1421* mutation blocks a significant increase in 16-18 splice isoforms that *smu-2* mutation would otherwise promote during larval development. On the other hand, *smu-2* mutation apparently leads to a significant decrease in an embryonically important splice form. One possibility, suggested previously for the effect of a *smu-1* mutation (43), is that *smu-2* mutation leads to a decrease in the 15-19 splice isoform, which is prominent in wild-type embryos (43) (data not shown). Since formation of splice isoforms that contain exon 16, including the embryonically abundant 16-19 isoform, is compromised in *e1421*, the level of functional *unc-52* transcripts in *smu-2 unc-52*(*e1421*) mutants could be inadequate to ensure normal embryonic development. Lethal interactions between the *smu-2* mutation and the remaining viable *unc-52* mutations may not occur because a decrease in the 15-19 splice isoform could be compensated for by an increase in the 16-19 splice isoform; the formation of both 15-19 and 16-19 isoforms is promoted by MEC-8 during embryogenesis (29, 34, 42).

***smu-2* probably affects the splicing of additional transcripts.** It was shown previously that *smu-2* mutations suppress, generally weakly, three distinct phenotypes or phenes conferred by mutations in *mec-8*: defects in mechanosensation, chemosensation, and embryogenesis at low temperature (28). It was concluded that these phenes are independent of *unc-52* action and are probably due to defects in the processing of additional pre-mRNA targets of MEC-8 action (29, 34). It was also concluded that the *smu-2* loss-of-function mutations exert their suppressing effects on the *mec-8* mutant phenes by providing a weak bypass function and not by partial restoration of MEC-8 activity (28), since all *mec-8* mutations that were tested, including those associated with presumed null alleles *u74*, *u456*, and *u391*, are partially suppressed by a *smu-2* mutation (28). The *u74* mutation results in an amino acid substitution at a highly conserved glycine residue in the first RRM domain of MEC-8, the *u456* mutation is a deletion that removes most of this domain, and the *u391* mutation is a complex rearrangement that produces no detectable MEC-8 (10, 42). The finding that loss of SMU-2 activity results in a partial bypass function led to the hypothesis that suppression by *smu-2* is due to loosened restrictions on wild-type patterns of splicing such that the loss of SMU-2 function leads to a low level of altered splice site choice that can partially compensate for the loss of MEC-8. Our results here on the effects of *smu-2* mutation on the splicing of *unc-52* pre-mRNA support this picture and strengthen our supposition that SMU-2 affects the splicing of additional MEC-8 targets, and perhaps non-MEC-8 targets as well. SMU-2's ubiquitous expression would be consistent with this picture.

On the other hand, if general splicing were grossly disturbed, we would expect *smu-2* mutants to be inviable, whereas they show only mild impairment in fertility and mild locomotory defects. None of our three mutant alleles has a null mutation, but putting a deletion mutation opposite that of one of our mutant alleles did not lead to a more severe phenotype, and *smu-2*(*RNAi*), which we showed was effective in reducing *smu-2* expression and in suppressing an *unc-52* mutation, had no effect on viability. We think it likely that the *smu-2* null phenotype is viable, as is the *smu-1* null phenotype (43), and that SMU-2 has mild effects on splicing, such as we saw for *unc-52* pre-mRNA splicing.

SMU-2 and SMU-1 bind to each other. Mutations in *smu-1* and *smu-2* behave identically in their patterns of suppression of *unc-52* and *mec-8* mutations and have identical effects on the pattern of *unc-52* splicing. Furthermore, *smu-1*; *smu-2* double mutants are phenotypically indistinguishable from each of the single mutants. These genetic arguments suggest that SMU-1 and SMU-2 exert their effects together, each being required for their combined wild-type function in controlling splicing. We also showed that mutation in *smu-2* decreases markedly the abundance of SMU-1 protein without altering the level of *smu-1* transcript, suggesting that SMU-2 is required to stabilize SMU-1. Consistent with this view is our finding, by both in vitro and in vivo assays, that SMU-1 and SMU-2 bind to each other. SMU-1 is a WD repeat protein (43). The canonical WD repeat protein, Gβ, is stabilized through a coiled-coil interaction at its N terminus with its partner Gγ (5, 41).

SMU-2 and SMU-1 are highly conserved spliceosome-associated proteins. We have found that SMU-2 is very similar to a mammalian protein named RED. SMU-2 and RED share amino acid sequence throughout their entire lengths, with 40% overall identity. RED appears to be a ubiquitously expressed nuclear protein (1), as is SMU-2. RED has been identified by two groups as a component of the human spliceosome (35, 52). SMU-2 is clearly its closest worm homolog. RED homologs are present in several other species, such as *D. melanogaster* and *A. thaliana*, but not in the budding yeast *Saccharomyces cerevisiae*, which does not carry out alternative splicing.

The RED protein is named for its outstanding feature, the RED domain, a region of residues with alternating charge—arginines alternating with glutamate or aspartate. The corresponding region in SMU-2 lacks glutamate but contains arginine alternating with aspartate or, occasionally, serine, making what we might refer to as an RD-RS hybrid domain. Other components of the spliceosome contain RD domains (44), including the U1 snRNP component U1 70K. The spliceosome also contains several proteins with RS domains, including the SR and SR-related protein families (13). The RS domains in SR proteins have a high degree of serine phosphorylation, which results in alternating charge, as in the RED and RD domains. RS domains are to some extent functionally interchangeable modules (47), and, in one case, an RS domain was replaced with an RD domain that provided the same function (6). The RS domain of SR proteins mediates protein-protein interaction (13). The function of the RED domain has not been studied, but the RED domain's similarity to an RS domain suggests that it too mediates protein-protein interaction. The *Arabidopsis* and *Drosophila* homologs seem to lack a RED domain altogether. Although we have performed secondary structure analyses on the sequences in the region of the RED domain in these homologs, we have not been able to find any conserved features among them.

The molecular identification of *smu-1* indicated that it encoded a protein that was 62% identical to a predicted human protein of unknown function (43). SMU-1 is, like SMU-2, a ubiquitously expressed nuclear protein. More recently, the predicted human SMU-1 homolog was found to be a component of the human spliceosome and was named fSAP57 for functional-spliceosome-associated protein 57 (52). SMU-1 is the only closely related worm homolog of fSAP57. In view of the high conservation of both SMU-1/fSAP57 and SMU-2/RED,

we propose that SMU-1 and SMU-2 in worms and fSAP57 and RED in humans work together in spliceosomes to mediate splice site choice.

How do SMU-2 and SMU-1 work? According to the picture that emerges, SMU-1 and SMU-2 work together to modulate, modestly, some but not all splice site choices. For *unc-52* transcripts, SMU-1 and SMU-2 are needed to decrease about twofold the skipping of exon 17 but do not affect the splicing of neighboring exons such as skipping of exon 18 (data not shown). This suggests that SMU-1 and SMU-2 discriminate among different RNA sequence elements. A single nucleotide change, the *su250* mutation, in the middle of intron 16 that alters the frequency of exon 17 skipping seems to lie in a *cis*-acting regulatory sequence (43). Regulatory sequences in both exons and introns that have either positive or negative effects on splicing have been identified in other systems (2). The discrimination of RNA sequence by SMU-1 and SMU-2 may well be indirect, involving other spliceosomal components, particularly since neither SMU-1 nor SMU-2 contains an apparent RNA binding motif. In addition, neither protein is expressed tissue specifically, and it seems unlikely that they regulate alternative splicing in a tissue-specific fashion. We suggest that they contribute to the wild-type fidelity of the spliceosome's action, such that their absence leads to alterations in splice site choice, which are only slightly harmful to the fitness of the organism.

Only a very small proportion of all spliceosomal proteins have had their functions tested in vivo by analysis of mutants. Fly SRp55 mutants (36) and mouse SRp20 mutants (20) are inviable, and RNAi has shown that SF1 (31), SF2/ASF (26, 53), and the U2 snRNP-specific proteins SAP49 (12), $U2AF^{35}$, and $U2AF^{65}$ (53) are essential in *C. elegans*. But RNAi treatment of SRm160 and five different SR protein genes in *C. elegans* (21, 26) resulted in no obvious phenotype, although subtle effects on splicing, as we have seen in *smu-1* and *smu-2* mutants, were not assayed. It has been suggested that many of the SR genes that gave no phenotype when treated singly by RNAi serve redundant functions because, when certain combinations of them were treated simultaneously by RNAi, lethal phenotypes were obtained (21, 26, 27). Targeting different combinations of SR genes for RNAi, however, yielded different developmental abnormalities, suggesting that different family members do not provide precisely overlapping functions. We imagine that inactivation of each spliceosomal protein may have an effect, if only a subtle one, and that the strong effects of multiple gene inactivation may be the consequence of multiple splicing errors. Of course there may also be synergistic effects in a multiply compromised spliceosome.

We do not know how SMU-1 and SMU-2 modulate splicing. Splice site choice seems often to be regulated by controlling the binding to the pre-mRNA of factors that influence assembly of early spliceosomal complexes. For example, the SR-related protein SRm160, which lacks RNA binding motifs (as do SMU-1 and SMU-2), is thought to act as a coactivator for certain splices by bridging interactions between other splicing factors, including U1 and U2 snRNP components (3). SMU-1 and SMU-2 might act similarly to favor inclusion of exon 17 of the *unc-52* transcript. They could do this either by promoting certain early complexes or by blocking others. A negative mode of action might be carried out by a region of SMU-2 that is rich in lysine and aspartic acid residues, an EK domain. The EK domain of SR-related protein SRrp86 was recently shown to regulate negatively both constitutive and alternative splicing (25). Finally, it is possible that SMU-1 and SMU-2 modulate a later catalytic step in the splicing reaction, as recently found for the *Drosophila* Sxl protein (23).

ACKNOWLEDGMENTS

We thank Heather Gardner and Dave Zarkower for *tim-1* and *tra-1* constructs, Y. Kohara for cDNA clones, and Todd Starich and John Yochem for much good advice. We give an especially big thanks to Caroline Spike for many useful discussions and technical guidance. Some nematode strains were provided by the Caenorhabditis Genetics Center.

This work was supported by U.S. National Institutes of Health (NIH) research grants GM22387 (R.K.H.) and GM56367 (J.E.S.). A.K.S. was a recipient of a doctoral dissertation fellowship from the University of Minnesota and a fellowship from NIH training grant HD07480.

REFERENCES

1. **Assier, E., H. Bouzinba-Segard, M. C. Stolzenberg, R. Stephens, J. Bardos, P. Freemont, D. Charron, J. Trowsdale, and T. Rich.** 1999. Isolation, sequencing and expression of RED, a novel human gene encoding an acidic-basic dipeptide repeat. Gene **230:**145–154.
2. **Black, D. L.** 2003. Mechanisms of alternative pre-messenger RNA splicing. Annu. Rev. Biochem. **72:**291–336.
3. **Blencowe, B. J., R. Issner, J. A. Nickerson, and P. A. Sharp.** 1998. A coactivator of pre-mRNA splicing. Genes Dev. **12:**996–1009.
4. **Brenner, S.** 1974. The genetics of *Caenorhabditis elegans* Genetics **77:**71–94.
5. **Bubis, J., and H. G. Khorana.** 1990. Sites of interaction in the complex between beta- and gamma-subunits of transducin. J. Biol. Chem. **265:**12995–12999.
6. **Cartegni, L., and A. R. Krainer.** 2003. Correction of disease-associated exon skipping by synthetic exon-specific activators. Nat. Struct. Biol. **10:**120–125.
7. **Chalfie, M., and M. Au.** 1989. Genetic control of differentiation of the *Caenorhabditis elegans* touch receptor neurons. Science **243:**1027–1033.
8. **Chan, R. C., A. Chan, M. Jeon, T. F. Wu, D. Pasqualone, A. E. Rougvie, and B. J. Meyer.** 2003. Chromosome cohesion is regulated by a clock gene paralogue TIM-1. Nature **423:**1002–1009.
9. **Dalton, S., and R. Treisman.** 1992. Characterization of SAP-1, a protein recruited by serum response factor to the c-fos serum response element. Cell **68:**597–612.
10. **Davies, A. G., C. A. Spike, J. E. Shaw, and R. K. Herman.** 1999. Functional overlap between the *mec-8* gene and five *sym* genes in *Caenorhabditis elegans*. Genetics **153:**117–134.
11. **Finney, M., and G. Ruvkun.** 1990. The *unc-86* gene product couples cell lineage and cell identity in *C. elegans*. Cell **63:**895–905.
12. **Fujita, M., T. Kawano, K. Terashima, Y. Tanaka, and H. Sakamoto.** 1998. Expression of spliceosome-associated protein 49 is required for early embryogenesis in *Caenorhabditis elegans*. Biochem. Biophys. Res. Commun. **253:**80–84.
13. **Graveley, B. R.** 2000. Sorting out the complexity of SR protein functions. RNA **6:**1197–1211.
14. **Hodgkin, J.** 1987. A genetic analysis of the sex-determining gene, *tra-1*, in the nematode *Caenorhabditis elegans*. Genes Dev. **1:**731–745.
15. **Hodgkin, J.** 1993. Molecular cloning and duplication of the nematode sex-determining gene, *tra-1*. Genetics **133:**543–560.
16. **Hresko, M. C., B. D. Williams, and R. H. Waterston.** 1994. Assembly of body wall muscle and muscle cell attachment structures in *Caenorhabditis elegans*. J. Cell Biol. **124:**491–506.
17. **Jakubowski, J., and K. Kornfeld.** 1999. A local, high-density, single-nucleotide polymorphism map used to clone *Caenorhabditis elegans cdf-1*. Genetics **153:**743–752.
18. **Jeon, M., H. F. Gardner, E. A. Miller, J. Deshler, and A. E. Rougvie.** 1999. Similarity of the *C. elegans* developmental timing protein LIN-42 to circadian rhythm proteins. Science **286:**1141–1146.
19. **Johnstone, I. L., and J. D. Barry.** 1996. Temporal reiteration of a precise gene expression pattern during nematode development. EMBO J. **15:**3633–3639.
20. **Jumaa, H., G. Wei, and P. J. Nielsen.** 1999. Blastocyst formation is blocked in mouse embryos lacking the splicing factor SRp20. Curr. Biol. **9:**899–902.
21. **Kawano, T., M. Fujita, and H. Sakamoto.** 2000. Unique and redundant functions of SR proteins, a conserved family of splicing factors, in *Caenorhabditis elegans* development. Mech. Dev. **95:**67–76.
22. **Krief, P., Y. Augery-Bourget, S. Plaisance, M. F. Merck, E. Assier, V. Tanchou, M. Billard, C. Boucheix, C. Jasmin, and B. Azzarone.** 1994. A new

cytokine (IK) down-regulating HLA class II: monoclonal antibodies, cloning and chromosome localization. Oncogene **9:**3449–3456.
23. **Lallena, M. J., K. J. Chalmers, S. Llamazares, A. I. Lamond, and J. Valcarcel.** 2002. Splicing regulation at the second catalytic step by Sex-lethal involves 3′ splice site recognition by SPF45. Cell **109:**285–296.
24. **Lewis, J. A., and J. T. Fleming.** 1995. Basic culture methods, p. 3–29. *In* H. F. Epstein and D. C. Shakes (ed.), *Caenorhabditis elegans*: modern biological analysis of an organism. Academic Press, San Diego, Calif.
25. **Li, J., D. C. Barnard, and J. G. Patton.** 2002. A unique glutamic acid-lysine (EK) domain acts as a splicing inhibitor. J. Biol. Chem. **277:**39485–39492.
26. **Longman, D., I. L. Johnstone, and J. F. Caceres.** 2000. Functional characterization of SR and SR-related genes in *Caenorhabditis elegans*. EMBO J. **19:**1625–1637.
27. **Longman, D., T. McGarvey, S. McCracken, I. L. Johnstone, B. J. Blencowe, and J. F. Caceres.** 2001. Multiple interactions between SRm160 and SR family proteins in enhancer-dependent splicing and development of *C. elegans*. Curr. Biol. **11:**1923–1933.
28. **Lundquist, E. A., and R. K. Herman.** 1994. The *mec-8* gene of *Caenorhabditis elegans* affects muscle and sensory neuron function and interacts with three other genes: *unc-52*, *smu-1* and *smu-2*. Genetics **138:**83–101.
29. **Lundquist, E. A., R. K. Herman, T. M. Rogalski, G. P. Mullen, D. G. Moerman, and J. E. Shaw.** 1996. The *mec-8* gene of *C. elegans* encodes a protein with two RNA recognition motifs and regulates alternative splicing of *unc-52* transcripts. Development **122:**1601–1610.
30. **Mackenzie, J. M., Jr., R. L. Garcea, J. M. Zengel, and H. F. Epstein.** 1978. Muscle development in *Caenorhabditis elegans*: mutants exhibiting retarded sarcomere construction. Cell **15:**751–762.
31. **Mazroui, R., A. Puoti, and A. Kramer.** 1999. Splicing factor SF1 from *Drosophila* and *Caenorhabditis*: presence of an N-terminal RS domain and requirement for viability. RNA **5:**1615–1631.
32. **Mello, C., and A. Fire.** 1995. DNA transformation, p. 451–482. *In* H. F. Epstein and D. C. Shakes (ed.), *Caenorhabditis elegans*: modern biological analysis of an organism. Academic Press, San Diego, Calif.
33. **Mello, C. C., J. M. Kramer, D. Stinchcomb, and V. Ambros.** 1991. Efficient gene transfer in *C. elegans*: extrachromosomal maintenance and integration of transforming sequences. EMBO J. **10:**3959–3970.
34. **Mullen, G. P., T. M. Rogalski, J. A. Bush, P. R. Gorji, and D. G. Moerman.** 1999. Complex patterns of alternative splicing mediate the spatial and temporal distribution of perlecan/UNC-52 in *Caenorhabditis elegans.* Mol. Biol. Cell **10:**3205–3221.
35. **Neubauer, G., A. King, J. Rappsilber, C. Calvio, M. Watson, P. Ajuh, J. Sleeman, A. Lamond, and M. Mann.** 1998. Mass spectrometry and EST-database searching allows characterization of the multi-protein spliceosome complex. Nat. Genet. **20:**46–50.
36. **Ring, H. Z., and J. T. Lis.** 1994. The SR protein B52/SRp55 is essential for *Drosophila* development. Mol. Cell. Biol. **14:**7499–7506.
37. **Rogalski, T. M., E. J. Gilchrist, G. P. Mullen, and D. G. Moerman.** 1995. Mutations in the *unc-52* gene responsible for body wall muscle defects in adult *Caenorhabditis elegans* are located in alternatively spliced exons. Genetics **139:**159–169.
38. **Rogalski, T. M., B. D. Williams, G. P. Mullen, and D. G. Moerman.** 1993. Products of the *unc-52* gene in *Caenorhabditis elegans* are homologous to the core protein of the mammalian basement membrane heparan sulfate proteoglycan. Genes Dev. **7:**1471–1484.
39. **Rose, A. M., and D. L. Baillie.** 1979. A mutation in *Caenorhabditis elegans* that increases recombination frequency more than threefold. Nature **281:** 599–600.
40. **Sambrook, J., E. F. Fritsch, and T. Maniatis.** 1989. Molecular cloning: a laboratory manual, 2nd ed. Cold Spring Harbor Laboratory Press, Plainview, N.Y.
41. **Schmidt, C. J., and E. J. Neer.** 1991. In vitro synthesis of G protein beta gamma dimers. J. Biol. Chem. **266:**4538–4544.
42. **Spike, C. A., A. G. Davies, J. E. Shaw, and R. K. Herman.** 2002. MEC-8 regulates alternative splicing of *unc-52* transcripts in *C. elegans* hypodermal cells. Development **129:**4999–5008.
43. **Spike, C. A., J. E. Shaw, and R. K. Herman.** 2001. Analysis of *smu-1*, a gene that regulates the alternative splicing of *unc-52* pre-mRNA in *Caenorhabditis elegans*. Mol. Cell. Biol. **21:**4985–4995.
44. **Staknis, D., and R. Reed.** 1995. Members of a family of proteins (the RD family) detected by a U1 70K monoclonal antibody are present in spliceosomal complexes. Nucleic Acids Res. **23:**4081–4086.
45. **Sulston, J., and J. Hodgkin.** 1988. Methods, p. 587–606. *In* W. B. Wood (ed.), The nematode *Caenorhabditis elegans*. Cold Spring Harbor Laboratory Press, Plainview, N.Y.
46. **Tyers, M., G. Tokiwa, R. Nash, and B. Futcher.** 1992. The Cln3-Cdc28 kinase complex of *S. cerevisiae* is regulated by proteolysis and phosphorylation. EMBO J. **11:**1773–1784.
47. **Wang, J., S. H. Xiao, and J. L. Manley.** 1998. Genetic analysis of the SR protein ASF/SF2: interchangeability of RS domains and negative control of splicing. Genes Dev. **12:**2222–2233.
48. **Williams, B. D., B. Schrank, C. Huynh, R. Shownkeen, and R. H. Waterston.** 1992. A genetic mapping system in *Caenorhabditis elegans* based on polymorphic sequence-tagged sites. Genetics **131:**609–624.
49. **Williams, B. D., and R. H. Waterston.** 1994. Genes critical for muscle development and function in *Caenorhabditis elegans* identified through lethal mutations. J. Cell Biol. **124:**475–490.
50. **Yochem, J., T. Gu, and M. Han.** 1998. A new marker for mosaic analysis in *Caenorhabditis elegans* indicates a fusion between hyp6 and hyp7, two major components of the hypodermis. Genetics **149:**1323–1334.
51. **Zarkower, D., and J. Hodgkin.** 1993. Zinc fingers in sex determination: only one of the two *C. elegans* Tra-1 proteins binds DNA in vitro. Nucleic Acids Res. **21:**3691–3698.
52. **Zhou, Z., L. J. Licklider, S. P. Gygi, and R. Reed.** 2002. Comprehensive proteomic analysis of the human spliceosome. Nature **419:**182–185.
53. **Zorio, D. A., and T. Blumenthal.** 1999. U2AF35 is encoded by an essential gene clustered in an operon with RRM/cyclophilin in *Caenorhabditis elegans*. RNA **5:**487–494.